Brain Radiation-Related Black Dots on Susceptibility-Weighted Imaging

DANIEL VARON, MICHAEL SIMONS, FRANCISCO CHIANG, GUSTAVO TEDESQUI, GERARDO PACHECO, PABLO MARTINEZ, MAURICIO CASTILLO

Department of Radiology, Neuroradiology Division, University of North Carolina at Chapel Hill; Chapel Hill, NC, USA

Key words: susceptibility-weighted imaging, radiation, MRI

SUMMARY – *Small blood vessel injury is a feature of post irradiation brain. Susceptibility weighted imaging (SWI) is a technique that exploits the magnetic properties of tissues, such as blood and iron content and is thus sensitive to hemorrhage as a marker of small vessel injury. Our purpose was to assess post irradiation brain findings using SWI. We evaluated 12 patients with follow-up MRI studies who underwent cranial irradiation for primary or metastatic tumors. From their clinical records, the latency interval, type of radiation, and total dose were established. The number and the distribution of "black dots" on SWI were analyzed. We also compared the findings on SWI with those seen on other MRI sequences. In all patients, black dots were clearly identified on SWI, while on conventional MRI (T2 and FLAIR) none were visible. Two patients with glial tumors received radiation with fields conforming to tumor beds, while all other patients received whole brain irradiation or craniospinal radiation. The total radiation doses ranged from 45-54 Gy. Latency interval between the time of irradiation and time of detection of the black dots was four to 60 months (mean, 31 months). In ten patients diffuse black dots were observed and in two patients these were located in the irradiated field. Black dots occurred in the cerebrum, cerebellum, and choroid plexuses. None of these dots showed enhancement. Follow-up in four patients showed that the numbers of these black dots had increased. Black dots were not present before radiation in any patient. Radiation-related black dots are an effect of cranial irradiation and may be related to small vessel damage. SWI is a sensitive technique for evaluation of these black dots.*

Introduction

Radiation therapy is the mainstay in the treatment of patients with primary and secondary intracranial tumors, however radiation has deleterious effects on the brain and a variety of radiation-induced changes occur. Radiation to the brain produces acute (during or shortly after radiation), early delayed (a few weeks to a few months post radiation), and late delayed changes (from several months to years after exposure) [1]. Common delayed effects of irradiation include diffuse white matter necrosis, focal or diffuse demyelination, reactive astrocytosis, brain atrophy, dystrophic mineralization, and radiation-induced vasculopathy [2]. Small-vessel injury is a prominent feature of delayed injury and different studies have shown that radiation can induce formation of capillary telangiectasias and cavernomas as a manifestation of vascular injury [3-8]. These vascular malformations could conceivably be confused with hemorrhagic metastases and their potential to bleed is unknown. Additionally, the relationship between them and post radiation cognitive impairment is uncertain. Thus, identifying them may well be the first step to understanding their clinical consequences.

Susceptibility-weighted imaging (SWI) is a technique that exploits the magnetic susceptibility differences of various tissues, such as blood, iron and calcification. It consists of using both magnitude and phase images from a high-resolution, three-dimensional (3D) fully velocity-compensated gradient echo sequence [11,12]. SWI is currently considered to be more sensitive than other conventional MRI techniques, including T2*-weighted imaging, for detection of hemor-

rhage [13]. With this new technique that has a greater sensitivity for detection of diamagnetic and paramagnetic substances, these sequelae are seen as "black dots" while they are not usually detected in conventional MRI sequences.

Multiple studies have evaluated hemorrhagic foci post radiation, but few have described the SWI findings following cranial irradiation. Here we used our initial experience with SWI to assess if these presumed post radiation vascular lesions can be seen with SWI, when they occur after treatment, and lastly which parts of the brain are affected by them.

Materials and Methods

The Institutional Committee for Medical Research Ethics approved this retrospective study and waived informed consent. A review of our records identified 12 patients studied between November 2012 and September 2013 who underwent cranial irradiation for primary or metastatic tumors and developed hypointense foci on SWI and who form the basis of this report.

MR imaging was performed on a 3T unit. Axial T2-weighted fast spin-echo imaging, axial T1-weighted imaging, axial fluid-attenuated inversion recovery imaging, DWI, and axial, coronal and sagittal T1 images after intravenous administration of 0.1-mmol/kg gadopentetate dimeglumine were available for all patients. SWI was obtained using a 3D spoiled gradient-recalled sequence with gradient moment nulling in all three orthogonal directions (64 sections per slab, FOV = 230 mm, matrix = 256 × 256, section thickness = 2 mm, voxel size = 0.9 × 0.9 × 2 mm, TE = 20 ms, TR = 28 ms, flip angle = 15°).

SWI data were processed off-line using software provided by the manufacturer. The purpose of post processing was to increase the conspicuity of magnetic susceptibility effects of tissue using the phase information. SWI was

Table 1 Demographics, clinical, and radiographic characteristics.

Case No.	*Sex*	*Age* (years)*	*Diagnosis*	*Radiation therapy*	*Total dose*	*Clinical presentation*	*Interval to SWI (months)*	*Location of black dots*	*Follow-up*
1	F	22	Medulloblastoma	Craniospinal radiation	45 GY	Incidental	23	Cerebrum, cerebellum	
2	M	6	Medulloblastoma	Craniospinal radiation	54 GY	Incidental	21	Cerebrum, cerebellum	
3	F	41	Breast metastasis	Whole brain	N/A	Incidental	N/A	Cerebrum	
4	M	10	Ependymoma	Whole brain	54 Gy	Incidental	45	Cerebrum, cerebellum	
5	M	8	Medulloblastoma	Craniospinal radiation	50 Gy	Incidental	24	Cerebrum, cerebellum	Increased in number
6	M	6	Ependymoma	Craniospinal radiation	N/A	Incidental	N/A	Cerebrum, cerebellum	
7	F	33	Medulloblastoma	Craniospinal radiation	54 Gy	Incidental	60	Cerebrum, cerebellum	Increased in number
8	M	37	Low grade glioma	Localized radiation	45 Gy	Incidental	22	Frontal, temporal	Increased in number
9	F	47	Breast metastasis	Whole brain	54 Gy	Incidental	36	Cerebrum, choroid plexuses	Increased in number
10	M	56	Oligoastrocitoma.	Localized radiation	54 Gy	Incidental	58	Right frontal	
11	M	13	Pineoblastoma	Craniospinal radiation	45 Gy	Incidental	4	Cerebrum	
12	F	20	Germ cell tumor	Craniospinal radiation	50 Gy	Incidental	29	Cerebrum, cerebellum	

Note. *Age* * indicates age at the time of detection of the black dots.

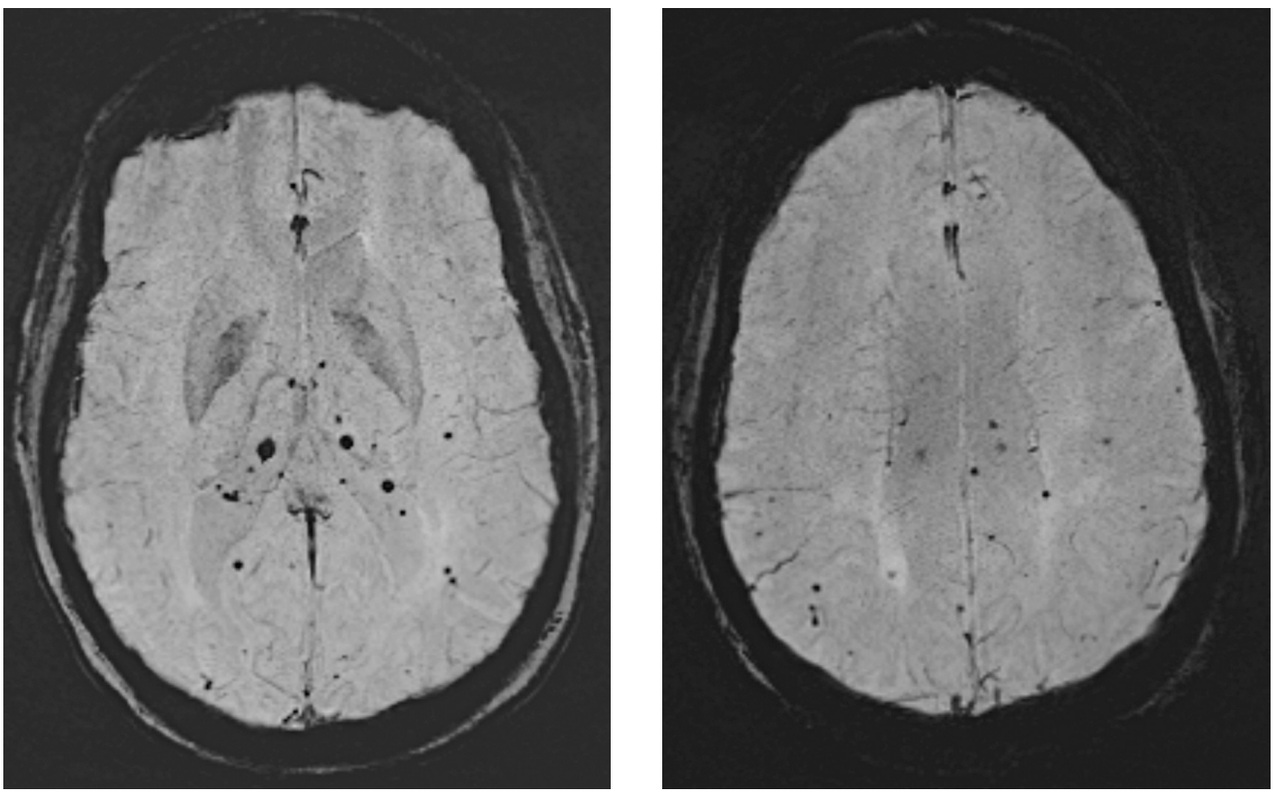

A B

Figure 1 Axial SWI demonstrates multiple black dots in the choroid plexi (A) and brain parenchyma (B) in a 43-year-old woman with previous metastases from breast cancer who underwent whole brain irradiation 36 months earlier. None of these lesions showed contrast enhancement (not shown).

created using both magnitude and phase images. A minimum intensity projection was performed to display the processed data.

Hypointense foci were determined to be present if small foci of very low signal intensity (black) were recognized on SWI. The presence of these hypointense foci, their size and distribution were evaluated by two neuroradiologists. T2 and FLAIR sequences were evaluated to determine if these foci were present on them and if associated findings were present. Post gadolinium imaging was evaluated in the location of the hypointense foci. If performed, subsequent follow-up MRI studies that included SWI were reviewed. From the clinical records, the symptoms, latency interval, type of radiation, and total dose were established. Pre-radiation studies were also assessed for the presence of black dots.

Analyses were conducted using SPSS version 20 (IBM, Armonk, NY, USA). Data were analyzed by using descriptive statistics and variables were expressed as means ± standard deviations.

Results

An overview of the results is given in Table 1. There were seven males and five females with an age range at the time of detection of the black dots of six to 56 years of age (mean: 23 years). Ten patients had primary central nervous system tumors and two patients had metastases. Ten patients received whole brain irradiation and/or craniospinal radiation while two received radiation with fields conforming to tumor beds with total radiation doses ranging from 45 to 54 Gy. In two patients the dates and doses of radiation could not be obtained. In the ten remaining patients, the latency interval between the time of irradiation and time of detection of the black dots was four to 60 months (mean: 32 months).

SWI hypointense foci were identified on routine surveillance imaging and no patients had symptoms thought to be related to them. In all patients, black dots were clearly identified on SWI, while on conventional MRI (T2

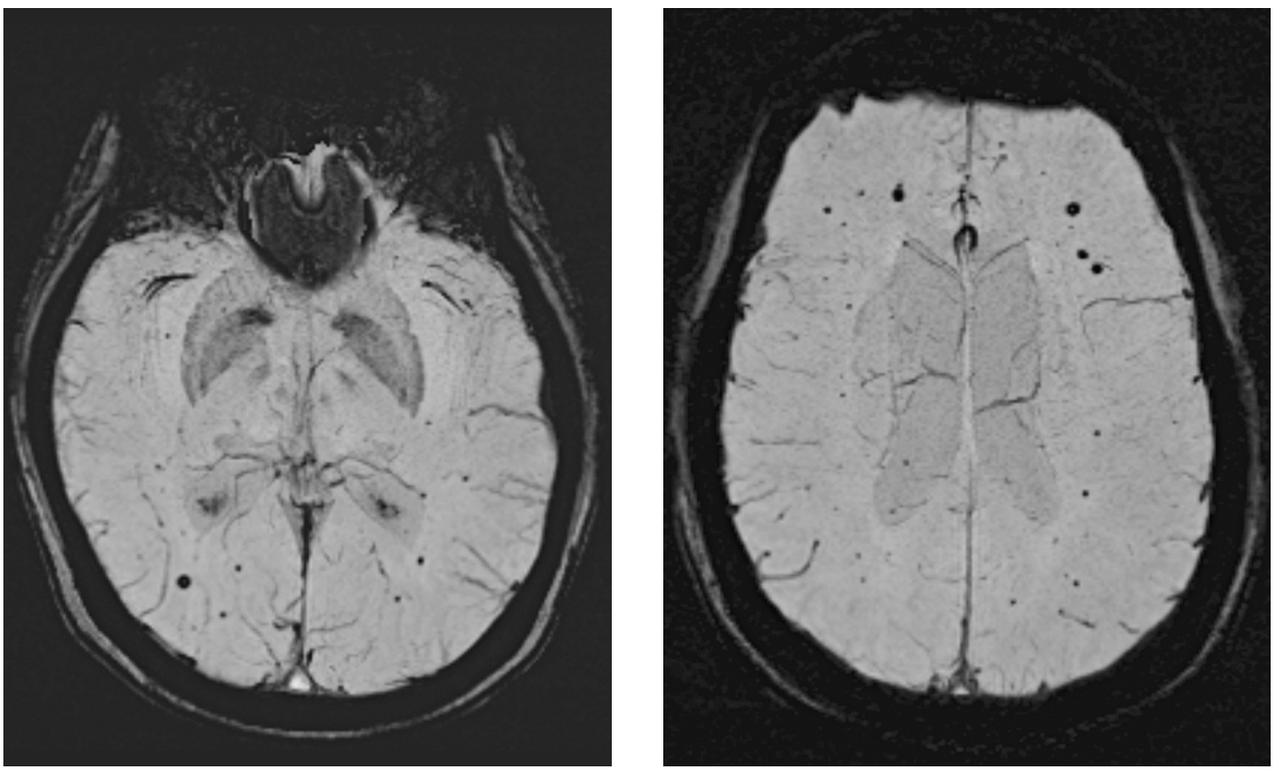

A B

Figure 2 (A,B) Axial susceptibility-weighted imaging (SWI). Multiple black dots are seen throughout the brain of a 22-year-old man who underwent craniospinal irradiation 23 months earlier for medulloblastoma.

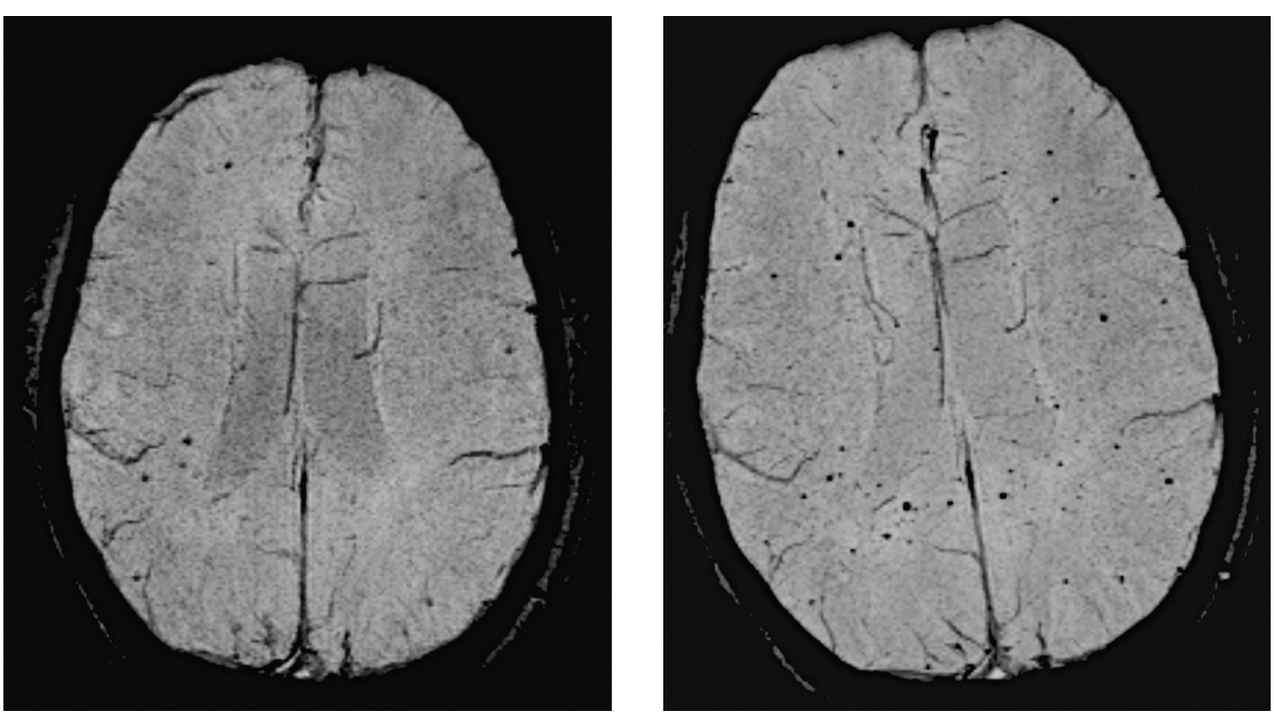

A B

Figure 3 Axial SWI. An 8-year-old boy with medulloblastoma who received craniospinal irradiation. The initial follow-up (A) demonstrates scattered foci of black dots; 18 months later the patient developed innumerable hypointense foci (B).

and FLAIR) none were visible. No surrounding edema or enhancement after gadolinium administration were observed related to these dark foci. The size of the black dots varied from 1-5 mm. In patients with whole brain irradiation and/or craniospinal irradiation, black dots were multiple and diffuse and were found in the brain, cerebellum and choroid plexi (Figures 1 and 2), while in the two patients with localized radiation the black dots were found in the irradiated field and immediately surrounding the original tumor site.

Eight patients had subsequent follow-up MRI studies that included SWI and the mean period of follow-up was 14 months (SD ± 4.15). In four patients the follow-up SWI showed that the black dots had increased in number as follows: in two patients their number tripled, in one patient doubled, and another patient who presented ten foci in the initial study later (20 months) developed innumerable dots (Figure 3). The mean time in which these new foci were identified during the follow-up was 15 months. No significant changes in size of the original lesions were demonstrated. Assessment of pretreatment MRI studies revealed that these black dots were not present at that time.

Discussion

Small vessel injury is related to progressive impaired cerebral microcirculation and is a prominent feature of delayed radiation injury. Different histologic manifestations of these vascular changes have been described, including endothelial injury and proliferation, fibrinoid necrosis, and induction of capillary telangiectasia and cavernomas [3,4,6].

Gaensler et al. [3] described the appearance of hemorrhagic foci on MRI following central nervous system irradiation. These hemorrhages ranged from small hypointense foci to larger regions of acute hemorrhage. Histopathologically specimens demonstrated clusters or foci of dilated small caliber vessels with thickened, hyalinized walls containing or surrounded by hemosiderin and these findings were attributed to radiation-induced telangiectasias. Therefore the distribution and pattern of hypointense foci on SWI may reflect hemorrhagic capillary telangiectasia.

Different studies report that radiation can induce formation of cavernomas and that this occurs at a significantly higher rate when patients are irradiated as children [4,6,7]. Cavernomas following radiotherapy are believed to result from injury to vascular structures because radiotherapy stimulates the upregulation of angiogenesis factors such as vascular endothelial growth factor and basic fibroblast growth factor. Stimulation of such growth factors normally found in cavernomas may explain increased cavernoma formation following radiotherapy [6,7]. A peripheral rim of hemosiderin surrounding a reticulated core of heterogeneous signal intensity are typical MRI features of cavernomas:because of the high sensitivity of SWI to blood products cavernomas may appear only as black dots and their central components may be overwhelmed by susceptibility effects and may not be visible. In our study none of the hypointense foci had the characteristic appearance of cavernomas but as explained above, we cannot exclude them. Studies have shown that many lesions that do not fulfill the diagnostic criteria for cavernomas on initial images do so in follow-up imaging [7]. In our eight follow-up patient, the nature of the black dots remained unchanged and thus we cannot confirm or exclude if they were cavernomas. In our patients all black dots had nonspecific appearances and showed no contrast enhancement or associated edema and since none had histopathologic confirmation their etiology remains uncertain.

We postulate that these hypointense foci may represent telangiectasias, small cavernomas, or microbleeds associated with both previously mentioned lesions and that the absence of enhancement makes it unlikely that they represent metastases.

SWI is exquisitely sensitive for detection of cerebral microhemorrhage with proven improved sensitivity over other techniques including T2 gradient echo imaging [13,14]. Recent studies found that the SWI frequency of microbleeds associated with radiation was higher than that reported in studies that used only conventional MRI sequences [9]. One study which included only conventional sequences showed that the frequency of radiation-induced telangiectasia was 20% [5] while in another study which used SWI it was 47% [9] Because of the retrospective nature of our study, it was not possible to determine the frequency of microbleeds in a large number of irradiated patients, but when comparing SWI with conventional sequences (T2 and FLAIR) the hypointense foci were clearly demonstrated and characterized in all patients with SWI while none was identified with other sequences.

The latency interval between time of irradiation and time of detection of black dots was 31 months on average but it is impossible to know when they appeared. Short latency periods between irradiation and appearance of black dots have been reported in previous studies [2,9]. It should be noted, that in one of our patients this latency was only four months suggesting that vascular injury may occur in the early post radiation period and not be restricted to delayed effects. The substantial increase in the number of microbleeds observed in four patients during the follow-up is not surprising considering that most vascular injury is known to happen months to years after treatment. These findings may also be related to the use of SWI in our study. A curious observation is that once established, these black dots do not grow in time suggesting that they may be hemorrhages rather than vascular malformations such as cavernomas which may grow, albeit slightly, as time passes.

From the clinical standpoint, in patients diagnosed with cancer and who have received whole brain irradiation, detection of new findings always raises the possibility that these could represent metastases or lead to a search of other possible causes that may result in changes in management. An important preliminary observation is that none of the black dots identified in our patients showed contrast enhancement leading us to suggest that they should not be considered de facto hemorrhagic metastases but rather the expected course of post radiation effects. More importantly, these black dots are clinically asymptomatic and no changes in management or interval of follow-up studies are needed.

Conclusion

Radiation-related black dots as seen on SWI are a common effect of cranial irradiation. SWI increases the conspicuity of these black dots presumably induced by radiation. The etiology of these black dots is uncertain and they could be related to microbleeds, capillary telangiectasias, and/or small cavernomas but they are unlikely to be metastases. Black dots appear to be asymptomatic.

References

1 Valk PE, Dillon WP. Radiation injury of the brain. Am J Neuroradiol. 1991; 12: 45-62.
2 Rabin BM, Meyer JR, Berlin JW, et al. Radiation-induced changes in the central nervous system and head and neck. Radiographics. 1996; 16: 1055-1072. doi: 10.1148/radiographics.16.5.8888390.
3 Gaensler EH, Dillon WP, Edwards MS, et al. Radiation-induced telangiectasia in the brain simulates cryptic vascular malformations at MR imaging. Radiology. 1994; 193: 629-636.
4 Jain R, Robertson PL, Gandhi D, et al. Radiation-induced cavernomas of the brain. Am J Neuroradiol. 2005; 26: 1158-1162.
5 Koike S, Aida N, Hata M, et al. Asymptomatic radiation-induced telangiectasia in children after cranial irradiation: frequency, latency, and dose relation. Radiology. 2004; 230: 93-99. doi: 10.1148/radiol.2301021143.
6 Heckl S, Aschoff A, Kunze S. Radiation-induced cavernous hemangiomas of the brain: a late effect predominantly in children. Cancer. 2002; 94: 3285-3291. doi: 10.1002/cncr.10596.
7 Burn, S, Gunny R, Phipps, K, et al. Incidence of cavernoma development in children after radiotherapy for brain tumors. J Neurosurg. 2007; 106: 379-383.
8 Keene DL, Johnston DL, Grimard L, et al. Vascular complications of cranial radiation. Childs Nerv Syst. 2006; 22: 547-555. doi: 10.1007/s00381-006-0097-4.
9 Tanino T, Kanasaki Y, Tahara T, et al. Radiation-induced microbleeds after cranial irradiation: evaluation by phase-sensitive magnetic resonance imaging with 3.0 Tesla. Yonago Acta Med. 2013; 56: 7-12.
10 Chung E, Bodensteiner J, Hogg JP. Spontaneous intracerebral hemorrhage: a very late delayed effect of radiation therapy. J Child Neurol. 1992; 7: 259-263. doi: 10.1177/088307389200700304.
11 Thomas B, Somasundaram S, Thamburaj K, et al. Clinical applications of susceptibility weighted MR imaging of the brain: a pictorial review. Neuroradiology. 2008; 50: 105-116. doi: 10.1007/s00234-007-0316-z.
12 Mittal S, Wu Z, Neelavalli J, et al. Susceptibility-weighted imaging: technical aspects and clinical applications, part 2. Am J Neuroradiol. 2009; 30: 232-252. Doi: 10.3174/ajnr.A1461.
13 Gao T, Wang Y, Zhang Z. Silent cerebral microbleeds on susceptibility-weighted imaging of patients with ischemic stroke and leukoaraiosis. Neurol Res. 2008; 30: 272-276. doi: 10.1179/016164107X251556.
14 Haacke EM, DelProposto ZS, Chaturvedi S, et al. Imaging cerebral amyloid angiopathy with susceptibility-weighted imaging. Am J Neuroradiol. 2007; 28: 316-317.
15 Sehgal V, Delproposto Z, Haacke EM, et al. Clinical applications of neuroimaging with susceptibility-weighted imaging. J Magn Reson Imaging. 2005; 22: 439-450. doi: 10.1002/jmri.20404.
16 Haacke EM, Mittal S, Wu Z, et al. Susceptibility-weighted imaging: technical aspects and clinical applications, Part I. Am J Neuroradiol. 2009; 30: 19-30. doi: 10.3174/ajnr.A1400.
17 Tong KA, Ashwal S, Obenaus A, et al. Susceptibility-weighted MR imaging: a review of clinical applications in children. Am J Neuroradiol. 2008; 29: 9-17. doi: 10.3174/ajnr.A0786.
18 Poussaint TY, Siffert J, Barnes PD, et al. Hemorrhagic vasculopathy after treatment of central nervous system neoplasia in childhood: diagnosis and follow-up. Am J Neuroradiol. 1995; 16: 693-699.
19 Del Curling O Jr, Kelly DL Jr, Elster AD, et al. An analysis of the natural history of cavernous angiomas. J Neurosurg. 1991; 75: 702-708. doi: 10.3171/jns.1991.75.5.0702.

Daniel Varon, MD
Department of Radiology, Neuroradiology Division
University of North Carolina at Chapel Hill
101 Manning Drive
Chapel Hill, NC 27514 United Status
E-mail: danielmvaron@hotmail.com